Scientific Papers of the
Institute of Electrical Power Engineering of the
Wrocław University of Technology

PRESENT PROBLEMS OF POWER SYSTEM CONTROL

No 1

Wrocław 2011

Keywords: wind generation, doubly-fed induction generator,
active and reactive power control,
stator flux reference frame

Leszek JEDUT*, Eugeniusz ROSOLOWSKI*

COMPARATIVE ANALYSIS OF POWER CONTROL SCHEMES IN DFIG FOR WIND ENERGY GENERATION

This paper describes two algorithms applied for active and reactive power control in wind turbine driven doubly fed induction generator (DFIG). The first proposed method applies the PI controllers for regulation of DFIG power and the rotor current while the second one utilizes a difference approximation of a given flux derivative. Both algorithms are based on the model description with reference to the stator flux linkage frame. General description of the analyzed methods is delivered and some results of simulations are included.

1. INTRODUCTION

The growing penetration of wind power on the electrical system and the increasing of the generating units rated power bring new challenges to the engineers. The wind-powered electricity generation grows rapidly because of the advantages of the active and reactive power regulate independently capacity and excitation converters requires small capacity, the doubly fed induction generator (DFIG) has been widely used in the wind power system. Due to an increase in the separate unit and total power of wind turbine installations, the utilities and the local network dispatchers request that wind supplied generators support the grid following different kind of disturbances.

Wind energy systems, generally, are based on variable-speed turbines. From among different alternatives to work with variable speed, the system based on the DFIG has been commonly employed for the recently build wind farms. In such a system the machine stator is directly connected to the grid and the rotor is connected via slip rings to a variable frequency inverter. To cover a wide range rotor speed - from

* Wroclaw University of Technology, Institute of Electrical Power Engineering, Wybrzeze Wyspianskiego 27, 50 – 370 Wroclaw, leszek.jedut@pwr.wroc.pl, rose@pwr.wroc.pl

subsynchronous to supersynchronous – the power converter needs to operate with power flowing in both directions (back-to-back inverter). For analyzing the mutual interaction between aforementioned wind generator and the utility network a simulation and modeling technique may be applied.

Traditionally, DFIG control is achieved by vector control (VC) [2], [4], which decouples the rotor currents into active power (or torque) and reactive power (or flux) components, and adjusts them separately in a reference frame fixed to either the rotor flux [4], the stator flux [7], [8], magnetizing flux [5] or voltage [4]. The rotor flux reference is calculated using the reactive power/power factor reference. Since the rotor supply frequency, can become very low, rotor flux estimation is significantly affected by the machine parameter variations. Recently, a direct power control strategy based on the estimated stator flux was proposed. Since the stator (network) voltage is relatively harmonic-free with fixed frequency, a DFIG's estimated stator flux accuracy can be guaranteed. The control system is very simple, and the machine parameters' impact on system performance was found to be negligible [7], [8]. The controller directly calculates the required rotor voltage within each fixed time period based on the stator flux, the rotor position, and the values of active and reactive powers and their errors. The very similar scheme based on the stator flux reference frame was proposed in [5]. The rotor current in *x*-*y* coordinates is used to control the stator reactive and active powers. The resulting control chain is composed of two control loops with two pairs of independent PI regulators: the inner one stabilizes the rotor current and the outer loop controls the value of active and reactive power.

In the paper two selected schemes for DFIG control are investigated by using of ATP-EMTP [1] and MATLAB-SIMULINK [3] models. Details of the proposed procedures are presented in the paper. Some results of simulations are also included.

2. DFIG MODEL DESCRIPTION

Considering the equivalent scheme of DFIG presented in Fig. 1 one can write the following relations for the stator and rotor voltages [6], [8]:

$$\underline{U}_s = -R_s \underline{I}_s + \frac{d\underline{\Psi}_s}{dt} + \mathrm{j}\omega_1 \underline{\Psi}_s \tag{1}$$

$$\underline{U}_r = R_r \underline{I}_r + \frac{d\underline{\Psi}_r}{dt} + \mathrm{j}\omega_{sl} \underline{\Psi}_r \tag{2}$$

where: ω_1 – angular velocity of the supplying voltage; $\omega_{sl} = \omega_1 - \omega_r$ – angular slip velocity; $\underline{U}_s = U_{sd} + \mathrm{j}U_{sq}$ and similarly for other vectors with:

$$\underline{\Psi}_s = L_m \underline{I}_r - L_s \underline{I}_s = L_m \underline{I}_m \tag{3}$$

$$\underline{\Psi}_r = L_r \underline{I}_r - L_m \underline{I}_s \tag{4}$$

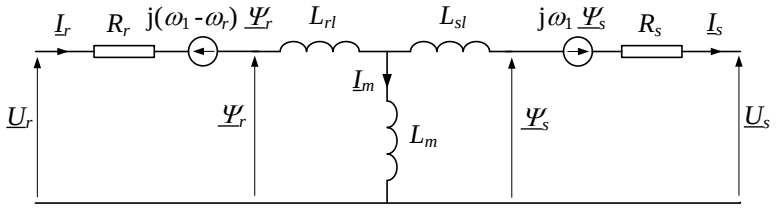

Fig. 1. Equivalent scheme of DFIG in synchronous *d-q* reference frame

The DFIG model defined by (1) and (2) in *d-q* reference frame is very important for further derivation because it assures the stator active and reactive power separate control by directing the current fed into the rotor windings [4], [7]. Let us track down the procedure to obtain the proper relations.

Neglecting of a zero-sequence component, the rotor and stator variables can be represented in their natural α-β frames by applying Clarke transformation:

$$\mathbf{X}_{\alpha\beta} = \mathbf{C}_1 \mathbf{X}_{\mathrm{ABC}} \tag{5}$$

where: $\mathbf{C}_1 = \frac{2}{3}\begin{bmatrix} 1 & -1/2 & -1/2 \\ 0 & \sqrt{3}/2 & -\sqrt{3}/2 \end{bmatrix}$, $\mathbf{X}_{\alpha\beta} = \begin{bmatrix} X_\alpha & X_\beta \end{bmatrix}^{\mathrm{T}}$, $\mathbf{X}_{\mathrm{ABC}} = \begin{bmatrix} X_A & X_B & X_C \end{bmatrix}^{\mathrm{T}}$.

In particular, the rotor current phasor components related to the rotor α-β frame are calculated as follows:

$$\mathbf{I}^r_{\mathrm{r}\alpha\beta} = \mathbf{C}_1 \mathbf{I}_{\mathrm{rABC}} \tag{6}$$

Therefore, the phasor $\underline{I}^r_{\mathrm{r}\alpha\alpha} = I^r_{r\alpha} + \mathrm{j}I^r_{r\beta}$ rotates in the angular velocity ω_r – the same as the rotor. It can be next transformed to the stator reference frame:

$$\underline{I}^s_{\mathrm{r}\alpha\beta} = \underline{I}^r_{\mathrm{r}\alpha\beta} \cdot \mathrm{e}^{\mathrm{j}\theta_r} \tag{7}$$

where θ_r is an angle between the rotor and the stator.

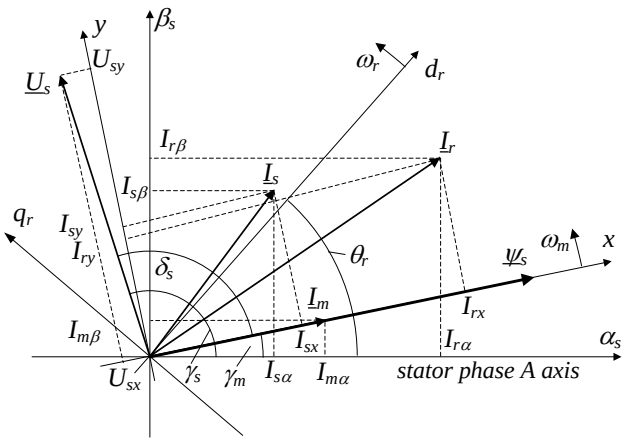

Fig. 2. Stator and rotor vectors

Having also the stator current determined in α-β coordinates (which can be calculated similarly as in (6)), a magnetizing current phasor can be given by [5]:

$$\underline{I}_{\mathrm{m}\alpha\beta} = \underline{I}^{s}_{r\alpha\beta} - \frac{L_s}{L_m}\underline{I}^{s}_{\mathrm{s}\alpha\beta} = I_{m\alpha} + \mathrm{j}I_{m\beta} = \left|I_m\right| \cdot \mathrm{e}^{\mathrm{j}\gamma_m} \tag{8}$$

where: $\gamma_m = \arctan\dfrac{I_{m\beta}}{I_{m\alpha}} = \displaystyle\int_0^t \omega_m dt + \gamma_{m0}$.

It can be noted that the angular velocity ω_m of the stator flux-linkage frame is practically the same as the velocity of the stator frame: $\omega_m \approx \omega_1$. The insignificant difference occurs only during a transient state and can be neglected. Therefore, the magnetizing current $\underline{I}_m$ in Fig. 1 is obtained from:

$$\underline{I}_m = \underline{I}_{\mathrm{mdq}} = \underline{I}_{\mathrm{m}\alpha\beta} \cdot \mathrm{e}^{-\mathrm{j}\gamma_m} \tag{9}$$

In fact, the stator flux-linkage frame is depicted as *x*-*y* frame, so similarly to (8) can be also transformed other variables of the DFIG model, e.g. transformation of the rotor current to the flux-linkage frame is given by:

$$\underline{I}_{\mathrm{rxy}} = \underline{I}^{s}_{\mathrm{rm}\alpha\beta}\mathrm{e}^{-\mathrm{j}\gamma_m} \tag{10}$$

It is interesting to note that in steady-state all variables related to the stator flux-linkage frame (*x*-*y* frame) take constant values.

To derive the rotor voltage control principle let us consider the flux linkage related to the *x-y* frame:

$$\underline{\Psi}_{xy} = L_m \underline{I}_{\mathrm{sxy}} = \underline{\Psi}^{s}_{\mathrm{sm}\alpha\beta} \mathrm{e}^{-j\gamma_m} \tag{11}$$

By definition the flux real component Ψ_x determines the 0*x* axis what gives:

$$\Psi_x = L_m I_{rx} - L_s I_{sx} = L_m \left|\underline{I}_m\right| \tag{12}$$

$$\Psi_y = L_m I_{ry} - L_s I_{sy} = 0 \tag{13}$$

It follows from (12), (13) that $I_{my} = 0$, $I_{mx} = \left|\underline{I}_m\right|$ and:

$$I_{sx} = \frac{L_m}{L_s}\left(I_{rx} - \left|I_m\right|\right), \quad I_{sy} = \frac{L_m}{L_s} I_{ry} \tag{14}$$

Substituting (11) – (14) into (2) and after adequate transformation yields:

$$\begin{aligned} U_{rx} &= U_{\mathrm{prx}} + U_{\mathrm{drx}} \\ U_{ry} &= U_{\mathrm{pry}} + U_{\mathrm{dry}} \end{aligned} \tag{15}$$

where:

$$\begin{aligned} U_{\mathrm{prx}} &= R_r I_{rx} + \sigma L_r \frac{dI_{rx}}{dt} \\ U_{\mathrm{pry}} &= R_r I_{ry} + \sigma L_r \frac{dI_{ry}}{dt} \end{aligned} \tag{16}$$

$$\begin{aligned} U_{\mathrm{drx}} &= -\omega_{sl} \sigma L_r I_{ry} \\ U_{\mathrm{dry}} &= \omega_{sl}(1-\sigma) L_r \left|I_m\right| + \omega_{sl} \sigma L_r I_{rx} \end{aligned} \tag{17}$$

and $\sigma = 1 - \dfrac{L_m^2}{L_s L_r}$.

The element $(1-\sigma)L_r\left(d\left|I_m\right|/dt\right)$ in (15) was omitted because changing of the magnetizing current magnitude is very small even during big disturbances [5].

It can be seen from (16), (17) that individual rotor voltage components depend on separate components of the rotor current. Expressions (16) represent differential equations which can be described in the Laplace transform notation:

$$I_{rx}(s) = \frac{1/R_r}{1+\sigma T_r s} U_{\text{prx}}(s)$$
$$I_{ry}(s) = \frac{1/R_r}{1+\sigma T_r s} U_{\text{pry}}(s) \tag{18}$$

where: $T_s = \frac{L_s}{R_s}$, $T_r = \frac{L_r}{R_r}$.

Adequate tuning of the rotor current components can be achieved by application of a PI regulator as in Fig. 3 [7]. Control schemes for both components are the same.

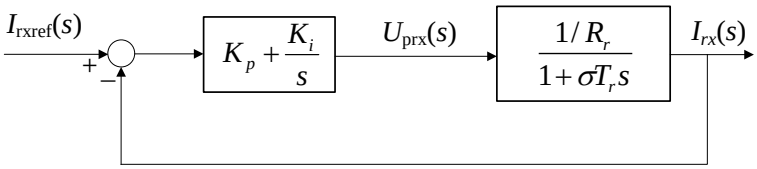

Fig. 3. Control scheme for adjusting the current I_{rx}

Settings of the PI controller in Fig. 3 can be calculated under the assumption that both coefficients K_p, K_i are related according to the rule:

$$K_p = \frac{K_i \sigma L_r}{R_r} \tag{19}$$

Under this condition the transfer function of the scheme from Fig. 3 is reduced to

$$G_{rx}(s) = \frac{I_{rx}(s)}{I_{\text{rx ref}}(s)} = \frac{1}{\tau_i s + 1} \tag{20}$$

where $\tau_i = R_r / K_i$ is a given time constant of the equivalent scheme from Fig. 3.

Starting from a given time constant τ_i the tuning PI controller coefficients are then determined as follows:

$$K_p = \frac{\sigma L_r}{\tau_i}, \quad K_i = \frac{R_r}{\tau_i} \tag{21}$$

The reference currents $I_{\text{rx ref}}, I_{\text{ry ref}}$ are defined by active and reactive powers control chain. Detailed formulas can be received on the basis of the stator:

$$\begin{aligned} P_s &= \frac{3}{2}\left(U_{sx}I_{sx} + U_{sy}I_{sy}\right) \approx \frac{3L_m}{2L_s}\left|\underline{U}_s\right| I_{ry} \\ Q_s &= \frac{3}{2}\left(U_{sy}I_{sx} - U_{sx}I_{sy}\right) \approx \frac{3L_m}{2L_s}\left|\underline{U}_s\right|\left(I_{rx} - \left|I_m\right|\right) \end{aligned} \tag{22}$$

and the rotor power components:

$$\begin{aligned} P_r &= -\frac{3}{2}\left(U_{rx}I_{rx} + U_{ry}I_{ry}\right) \\ Q_r &= -\frac{3}{2}\left(U_{ry}I_{rx} - U_{rx}I_{ry}\right) \end{aligned} \tag{23}$$

Total power components delivered to the network are:

$$P_n = P_s + P_r, \quad Q_n = Q_s + Q_r \tag{24}$$

Proceeding similarly as for the current control loop the following transfer function for equivalent active power control chain may be obtained (Fig. 4):

$$G_P(s) = \frac{P_n(s)}{P_{\text{nref}}(s)} = \frac{\dfrac{K_{1p}}{\tau_i}\left(s + \dfrac{1}{\tau_i}\right)}{s^2 + \dfrac{1 + K_{1p}B_s}{\tau_i}s + \dfrac{K_{1i}B_s}{\tau_i}} \tag{25}$$

where $B_s = \dfrac{3L_m U_s}{2L_s}$ is the scaling factor.

Transfer function (25) can also be reduced to the first order element under the assumption: $K_{1p} = K_{1i}\tau_i$. Then (25) is simplified to:

$$G_P(s) = \frac{P_n(s)}{P_{\text{nref}}(s)} = \frac{1}{\tau_i B_s\left(s\tau_1 + 1\right)} \tag{26}$$

For a given time constant τ_1 the PI_1 controller parameters are as follows:

$$K_{1i} = \frac{1}{B_s\tau_1}, \quad K_{1p} = \frac{\tau_i}{B_s\tau_1} \tag{27}$$

It can be noted that the gain in the equivalent control loop as in Fig. 4 is equal to: $k=(1/B_s\tau_i)$ (26). This derivation can be repeated for reactive power control loop receiving the same results. Time constant τ_i and τ_1 should be selected small to obtain fast response but not too very small to avoid a noise influence.

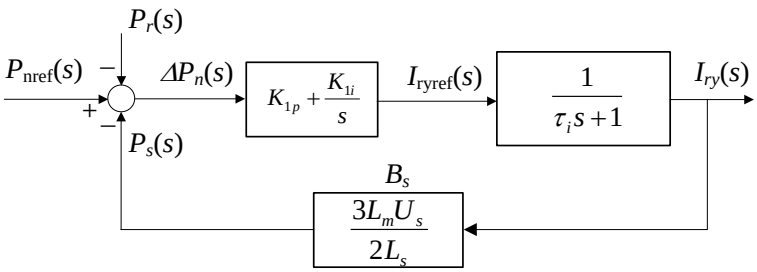

Fig. 4. Control loop for the active power adjusting the current I_{rx}

Relations (15)-(17) with the PI controllers description define the first considered algorithm for DFIG control.

The second regarded algorithm is based on the assumption that the integration operation in the PI controller is replaced by adequate difference calculus [8], [9]. Considering the formula (2) with respect to the flux derivative one can write the following change of this flux during sampling period T_s:

$$\Delta\underline{\Psi}_r=(\underline{U}_r-R_r\underline{I}_r-\mathrm{j}\omega_{sl}\underline{\Psi}_r)T_s \tag{28}$$

The stator power can be determined from the relation:

$$P_s-\mathrm{j}Q_s=\frac{3}{2}\underline{U}_s\underline{I}_s^* \tag{29}$$

Taking into account (3) and (4) and neglecting the voltage drop on the stator and rotor resistances the above expression may be written in the forms:

$$P_s=k_\sigma\left(\Psi_{sd}\left(\Psi_{rq}-\frac{L_r}{L_m}\Psi_{sq}\right)-\Psi_{sq}\left(\Psi_{rd}-\frac{L_r}{L_m}\Psi_{sd}\right)\right) \tag{30}$$

$$Q_s=k_\sigma\left(\Psi_{sd}\left(\Psi_{rd}-\frac{L_r}{L_m}\Psi_{sd}\right)+\Psi_{sq}\left(\Psi_{rq}-\frac{L_r}{L_m}\Psi_{sq}\right)\right) \tag{31}$$

where: $k_\sigma = \dfrac{3L_m\omega_1}{2\sigma L_s L_r}$.

Rearranging of (30), (31) leads to:

$$\Psi_{rd} = \frac{1}{k_\sigma \left|\underline{\Psi}_s\right|^2}\left(\Psi_{sd}Q_s - \Psi_{sq}P_s\right) + \frac{L_r}{L_m}\Psi_{sd} \tag{32}$$

$$\Psi_{rq} = \frac{1}{k_\sigma \left|\underline{\Psi}_s\right|^2}\left(\Psi_{sq}Q_s + \Psi_{sd}P_s\right) + \frac{L_r}{L_m}\Psi_{sq} \tag{33}$$

Changing of active and reactive powers on ΔP_s, ΔQ_s values, respectively, results in adequate changing of the rotor fluxes:

$$\Delta\Psi_{rd} = \frac{1}{k_\sigma \left|\underline{\Psi}_s\right|^2}\left(\Psi_{sd}\Delta Q_s - \Psi_{sq}\Delta P_s\right) \tag{34}$$

$$\Delta\Psi_{rq} = \frac{1}{k_\sigma \left|\underline{\Psi}_s\right|^2}\left(\Psi_{sq}\Delta Q_s + \Psi_{sd}\Delta P_s\right) \tag{35}$$

Adequate substitution of components from (28) into (34) and (35), with application of (32) and (33) gives similar relations as in (15):

$$\begin{aligned} U_{rd} &= U_{\mathrm{prd}} + U_{\mathrm{drd}} \\ U_{rq} &= U_{\mathrm{prq}} + U_{\mathrm{drq}} \end{aligned} \tag{36}$$

where:

$$\begin{aligned} U_{\mathrm{prd}} &= \frac{1}{k_\sigma \left|\underline{\Psi}_s\right|^2 T_s}\left(\Psi_{sd}\Delta Q_n - \Psi_{sq}\Delta P_n\right) \\ U_{\mathrm{prq}} &= \frac{1}{k_\sigma \left|\underline{\Psi}_s\right|^2 T_s}\left(\Psi_{sq}\Delta Q_n + \Psi_{sd}\Delta P_n\right) \end{aligned} \tag{37}$$

$$\begin{aligned} U_{\mathrm{drd}} &= -\omega_{sl}\left(\frac{1}{k_\sigma \left|\underline{\Psi}_s\right|^2}\left(\Psi_{sq}Q_n + \Psi_{sd}P_n\right) + \frac{L_r}{L_m}\Psi_{sq}\right) + R_r I_{rd} \\ U_{\mathrm{drq}} &= \omega_{sl}\left(\frac{1}{k_\sigma \left|\underline{\Psi}_s\right|^2}\left(\Psi_{sd}Q_n - \Psi_{sq}P_n\right) + \frac{L_r}{L_m}\Psi_{sd}\right) + R_r I_{rq} \end{aligned} \tag{38}$$

Relations (36) – (38) constitute the considered second algorithm. It is demonstrated in the next section that both considered algorithms have almost the same characteristics.

3. EXPERIMENTAL RESULTS

Simulations were provided by utilizing of ATP-EMTP [1] and MATLAB – SIMULINK [3]. In the last case also AC/DC/AC SVM electronic converter was included. Parameters of the investigated DFIG are presented in Table 1.

Table 1. DFIG parameters

Parameter	Description	Value
R_s	stator resistance	1.717 mΩ
R_r	rotor resistance	5.563 mΩ
L_s/ L_r	stator/rotor inductance per phase	2.409 mH
L_m	magnetizing inductance	2.354 mH
p	number of pole pairs	2
$\|U_s\|$	stator voltage peak value	690√2/√3
S_n	nominal power	2.5 MVA

Some results of simulations of the considered DFIG with utilizing ATP-EMTP model (without electronic converters) are presented in Figs. 5 and 6. Parameters of PI controllers are assumed as follows: τ_i = 0.02s and τ_1 = 0.03s. The given powers: P_{nref} and Q_{nref} are abruptly changed as in Fig. 5. It can be seen that the obtained powers accurate tracing the given waveforms – both algorithms give almost the same results. The accompanying rotor phase current waveforms are presented in Fig. 6. These waveforms are almost the same for both analyzed algorithms.

In Fig. 7, the typical connection scheme is presented. The stator windings are directly connected to the line grid, while the rotor windings are supplied by a bidirectional power converter. The aim of the rotor side converter is to control independently active and reactive power on the grid and grid side converter has to keep the dc link capacitor voltage at the set value.

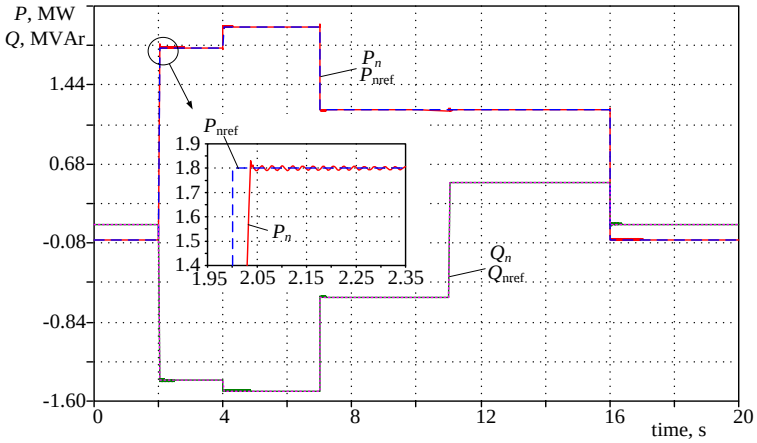

Fig. 5. Changing of active and reactive power in ATP-EMTP model

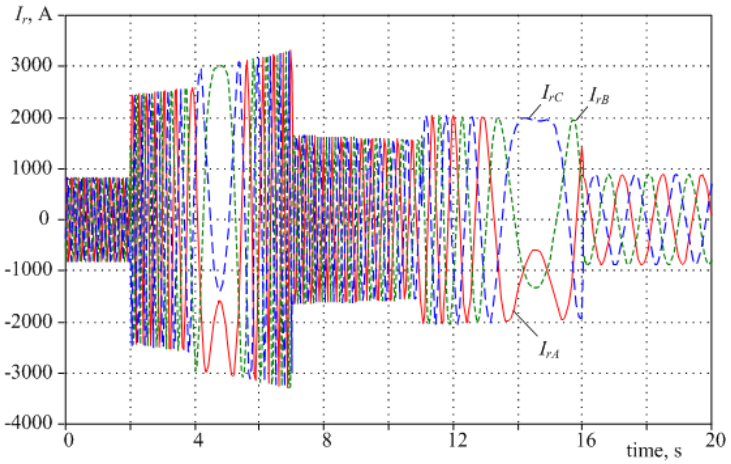

Fig. 6. The rotor current waveforms during test as in Fig. 5

Figs. 8-10 present some results of simulation which was executed in Matlab/Simulink. The model consist of full electronics converter (grid-side converter - GSC and rotor-side converter - RSC), so one can see small differences between settings value of P_{nref} and Q_{nref} and that obtained at the output of the machine: active power P_n and reactive power Q_n.

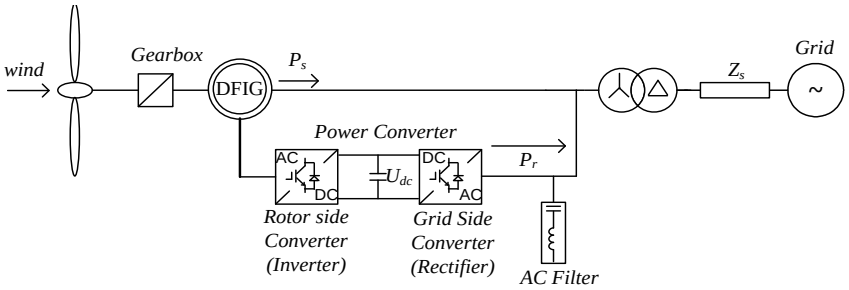

Fig. 7. Scheme of wind generation unit with DFIG

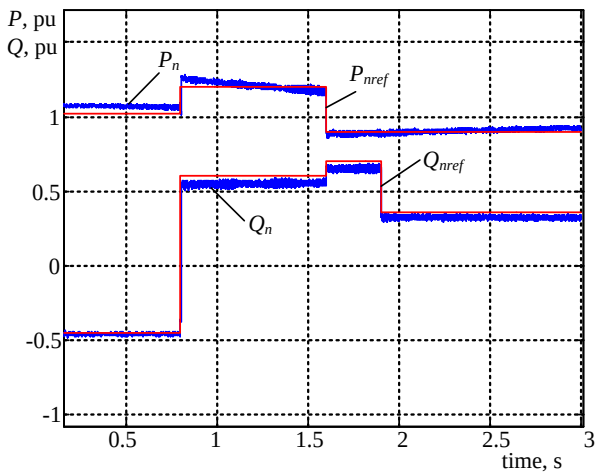

Fig. 8. Changing of active and reactive power in MATLAB/SIMULINK model

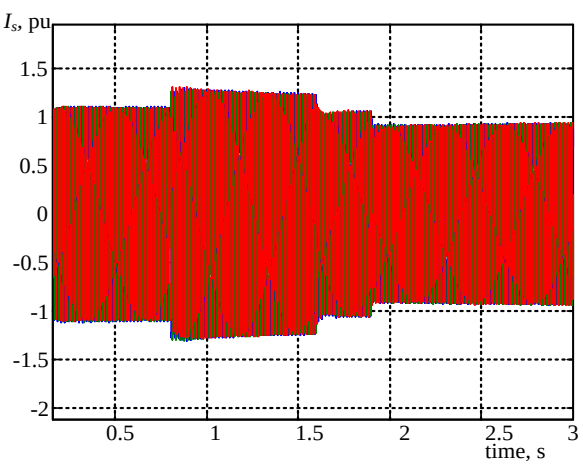

Fig. 9. The stator current waveforms during test as in Fig. 8

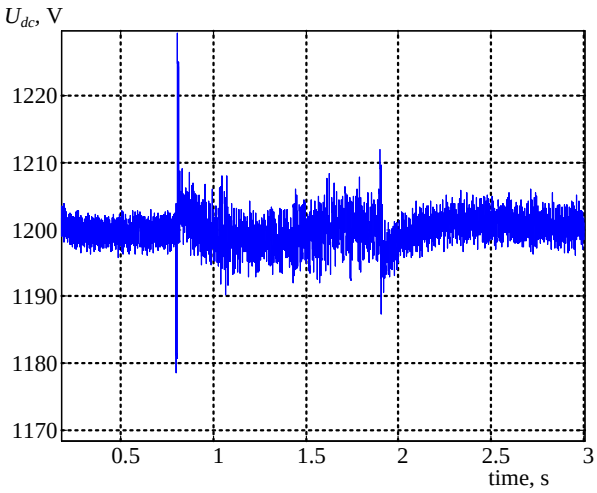

Fig. 10. Voltage U_{dc} waveform during test as in Fig. 8

Analyzing results from Figs. 8 and 9 one can observe that they follow the DFIG mathematical model: according to (14), the stator current are proportional to rotor current and rotor current depends on active and reactive power as in (22). When active and reactive powers increase, stator current raises too. Regulator of grid side converter (not describing here) keeps dc link in the constant value even during severe changing of power. Nominal voltage for dc link is equal to 1200 V.

4. CONCLUSIONS

A control structure and design of active and reactive power controllers applied in wind turbine driven DFIG was presented. The proposed schemes apply well-known linear control techniques. The algorithms were implemented in simulation models prepared in ATP-EMTP and MATLAB/SIMULINK programs. For simplicity the ATP-EMTP model was reduced: voltage sources in the rotor circuit were represented by controlled voltage. In MATLAB/SIMULINK program there was applied full power converter. Results of simulation confirm that both analyzed methods operate correctly and give similar results.

ACKNOWLEDGMENT

This work has been supported by the government of the Republic of Poland, Research Project No N N5111 352237.

REFERENCES

[1] DOMMEL H., *Electro-Magnetic Transients Program*, BPA, .Portland, Oregon, 1986
[2] MALINOWSKI M., JASINSKI M., KAZMIERKOWSKI M.P., *Simple direct power control of three-phase PWM rectifier using space-vector modulation (DPC-SVM)*. IEEE Trans. Ind. Electron, Vol. 51, no. 4, pp. 447–454, Apr. 2004.
[3] MATHWORKS, *Simulink 7.2*. Available in: http://www.mathworks.com/products/simulink/
[4] PENA R., CLARE J.C., ASHER G.M., *Double fed induction generator using back-to-back PWM converter and its application to variable- speed wind-energy generation.* IEE Proc.-Electr. Power Appl., Vol. 143, no. 3, pp. 231–241, 1996.
[5] TAPIA A., TAPIA G., OSTOLAZA J.X., SAENZ J.R., *Modeling and Control of a Wind Turbine Driven Doubly Fed Induction Generator*. IEEE Trans. Energy Convers., Vol. 18, No. 2, pp. 194–204, June 2003.
[6] TAPIA G., SANTAMARIA G., TELLERIA M., SUSPERREGUI A., *Methodology for Smooth Connection of Doubly Fed Induction Generators to the Grid*. IEEE Trans. Energy Convers., Vol. 24, No. 4, pp. 959–971, December 2009.
[7] VAS P., *Sensorless Vector and Direct Torque Control*. Oxford University Press, Oxford, U.K., 1998.
[8] XU L., CARTWRIGHT P., *Direct active and reactive power control of DFIG for wind energy generation.* IEEE Trans. Energy Convers., Vol. 21, No. 3, pp. 750–758, September 2006.
[9] ZHI D., XU L., *Direct power control of DFIG with constant switching frequency and improved transient performance.* IEEE Trans. Energy Convers., Vol. 22, No. 1, pp. 110–118, March 2007.

ANALIZA PORÓWNAWCZA METOD STOSOWANYCH DO REGULACJI MOCY CZYNNEJ I BIERNEJ W DWUSTRONNIE ZASILANYM GENERATORZE INDUKCYJNYM

W artykule przedstawiona jest analiza dwóch algorytmów stosowanych do regulacji mocy czynnej i biernej w elektrowniach wiatrowych z dwustronnie zasilanymi generatorami indukcyjnymi. W pierwszej rozważanej metodzie stosowane są regulatory PI do kontroli mocy i prądu wirnika, podczas gdy w drugiej - całkowanie ciągłe jest aproksymowane za pomocą zależności przyrostowych. W obu algorytmach model maszyny jest zapisany względem układu współrzędnych związanych ze strumieniem stojana. Zamieszczony jest opis rozważanych modeli oraz wyniki przeprowadzonych symulacyjnych testów.